Medical Engineering & Physics 32 (2010) 1107–1115

Contents lists available at ScienceDirect

Medical Engineering & Physics

journal homepage: www.elsevier.com/locate/medengphy

# Non-invasive assessment of corneal endothelial permeability by means of electrical impedance measurements

A. Guimera[a,b,*], A. Ivorra[c], G. Gabriel[a,b], R. Villa[a,b]

[a] Instituto de Microelectrónica de Barcelona, IMB-CNM (CSIC), Campus UAB, 08193 Bellaterra, Barcelona, Spain
[b] Networking Research Center on Bioengineering, Biomaterials and Nanomedicine (CIBER-BBN), Campus UAB, 08193 Bellaterra, Barcelona, Spain
[c] Department of Information and Communication Technologies, Universitat Pompeu Fabra, Carrer Tánger 122-140, 08018 Barcelona, Spain

ARTICLE INFO

*Article history:*
Received 16 March 2010
Received in revised form 26 July 2010
Accepted 26 July 2010

*Keywords:*
Electrical impedance spectroscopy
Corneal endothelium
Permeability
Finite elements method

ABSTRACT

The permeability of the corneal endothelial layer has an important role in the correct function of the cornea. Since ionic permeability has a fundamental impact on the passive electrical properties of living tissues, here it is hypothesized that impedance methods can be employed for assessing the permeability of the endothelial layer in a minimally invasive fashion. Precisely, the main objective of the present study is to develop and to analyze a minimally invasive method for assessing the electrical properties of the corneal endothelium, as a possible diagnostic tool for the evaluation of patients with endothelial dysfunction. A bidimensional model consisting of the main corneal layers and a four-electrode impedance measurement setup placed on the epithelium has been implemented and analyzed by means of the finite elements method (FEM). In order to obtain a robust indicator of the permeability of the endothelium layer, the effect of the endothelium electrical properties on the measured impedance has been studied together with reasonable variations of the other model layers. Simulation results show that the impedance measurements by means of external electrodes are indeed sufficiently sensitive to the changes in the electrical properties of the endothelial layer. It is concluded that the method presented here can be employed as non-invasive method for assessing endothelial layer function.



## 1. Introduction

Although corneal surgery and disease are very common, there is a lack of proper non-invasive diagnostic methods for determining the suitability of a given patient for a corneal surgical procedure that may weaken the cornea or for assessing the suitability of a donor cornea for transplantation.The cornea (Fig. 1) is a transparent hemispherical structure located in front of the eye that allows the transmission of light. Basically, it consists of three layers: the epithelium, the stroma and the endothelium. To maintain transparency the cornea does not have capillaries for supplying nutrients, they are supplied by diffusion through the epithelium and endothelium. The transparency of the cornea depends on the level of hydration of the stroma, remaining in a constant state of dehydration. As shown in Fig. 2, the hydration level of the stroma depends mainly of three different ion fluxes. Two of those fluxes are due to diffusion: one between tear layer and stroma through the epithelium and another one between stroma and aqueous humor through the endothelium. Finally, an active flux is due to fluid pump through the endothelium cells. The endothelium is a monolayer of cells without regenerative capacity and plays the most important role for maintaining the low hydration rate of the stroma and consequently the transparency of the cornea [1,2].The corneal endothelium morphology and its physiopathological status can be evaluated in the clinical practice by several techniques. Indirect methods as endothelial fluorophotometry [3] and pachymetry [4] are unreliable for monitoring individual patient changes [5]. On the other hand, specular microscopy [6] and confocal microscopy are direct methods only suitable for the examination of corneal endothelium morphology [7]. The endothelial cell density is the most widely used parameter for assessing the suitability of a cornea to be transplanted. But, a recent study concludes that the preoperative value of this parameter is unrelated to graft failure due to endothelial decomposition, whereas there is a strong correlation of this parameter at 6 months [8]. The barrier effect of the cornea can be assessed by the study of their passive electrical properties. Transendothelial electric resistance (TER) method is consistently used in *in vitro* studies for assessing the permeability of the corneal endothelium [9,10]. Studies using TER measurements in *in vivo* setups [11,12] are out of consideration for clinical methods due to their invasiveness.Here is proposed that it is possible to assess corneal endothelium permeability by means of non-invasive impedance measurements

* Corresponding author at: Instituto de Microelectrónica de Barcelona, IMB-CNM (CSIC), Campus UAB, 08193 Bellaterra, Barcelona, Spain. Tel.: +34 935947700.
*E-mail address:* anton.guimera@imb-cnm.csic.es (A. Guimera).

1350-4533/$ – see front matter © 2010 IPEM. Published by Elsevier Ltd. All rights reserved.
doi:10.1016/j.medengphy.2010.07.016

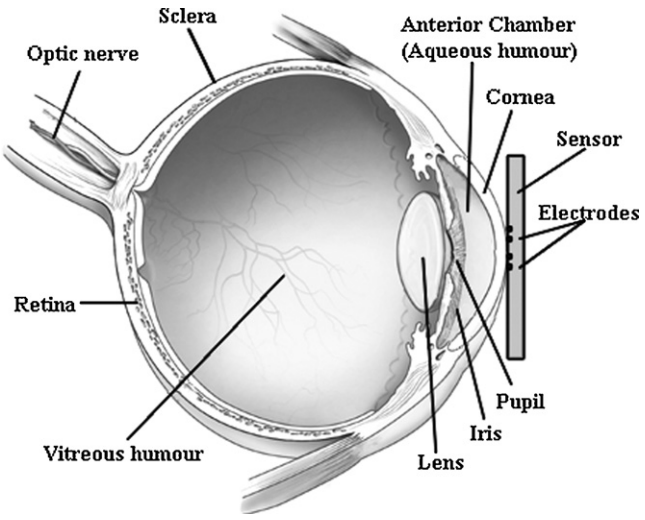


**Fig. 1.** Schematic representation of the ocular globe, which shows the location of the main parts and the position of the proposed sensor.

performed with electrodes placed on the surface of the cornea, as illustrated in Fig. 1. For analyzing the feasibility of the proposed method, and for finding which impedance parameters are better suited for such purpose, a numerical study has been carried out. This numerical study is based on simulations performed using the finite elements method (FEM); an electrical model of the main cornea layers was built and the corresponding electrical properties were selected from data reported in the literature. In particular, endothelial permeability was modeled as a variation of its conductivity. The simulated conductivity variations were based on experimental measurements made in a number of *in vitro* studies.

## 2. Methods

### 2.1. Simulation model

FEM modeling has been used for investigating the current and the potential distributions in the cornea in the case of impedance measurements made with the four-electrode method. In particular, modeling has been carried out by employing the commercial FEM tool COMSOL Multiphysics 3.4 and its associated application mode "Quasi-statics, Electric" of the "AC/DC module".

The four-electrode method here considered, compared to the more common two-electrode method, offers the advantage of minimizing, and ideally cancelling, the parasitic effects of the electrode–electrolyte interface impedances [13]. The impedance has been calculated using Ohm's law, $Z = V/I$. In the simulations, a constant AC current has been injected through the outer electrodes ($I+$ and $I-$) and the inner electrodes ($V+$ and $V-$) have been used to sense the voltage drop. The electrodes have been modeled with a very high conductivity ($6 \times 10^7$ S/m) so that the voltage in all points of the electrode is the same. The outer boundaries of the model have been defined as electric insulation, in other words, no current can flow through them. These boundaries have been placed far enough from the electrodes (5 mm) so that it can be considered that the current density in this zone is very low and, therefore, the effect of the tissues located near these boundaries in the impedance measurements is negligible.

Fig. 3 shows the model used that is formed by the three main layers of the cornea and the electrodes, and takes into account the surrounding fluids like tear and aqueous humor. Assuming that the length of the electrodes is much greater than their width, only a vertical cross-section of the layers needs to be modeled [14]. This fact simplifies the computational model because it can be reduced in one dimension, from 3D to 2D. Using this model, a 2D analysis within frequency range from 10 Hz to 1 MHz has been carried out. Two sets of electrodes have been tried in this study, in order to find the better configuration for detecting changes in the passive electrical properties of the endothelium layer. Fig. 3 shows the geometry of the used electrode sets. In both electrode sets, the ratio of the separation between the electrodes is the same; it is the total sensor width that is different between both sets (3 mm and 5 mm). In particular, the distance between inner electrodes is three times larger than the separation between the outer electrodes. This ratio of distances offers some advantages in terms of spatial resolution [15,16]. The sensor width is related to the "penetration" of the measurement; it is advantageous to maximize this parameter in order to ensure that much of current goes through the endothelium layer. On the other hand, the sensor width is limited by the dimensions

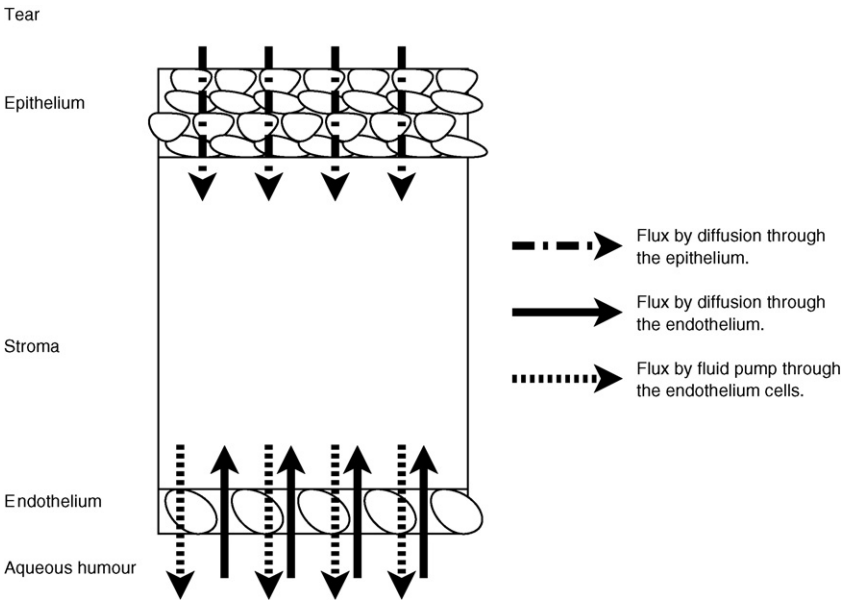


**Fig. 2.** Schematic representation of the main layers of the cornea and the main ion fluxes.

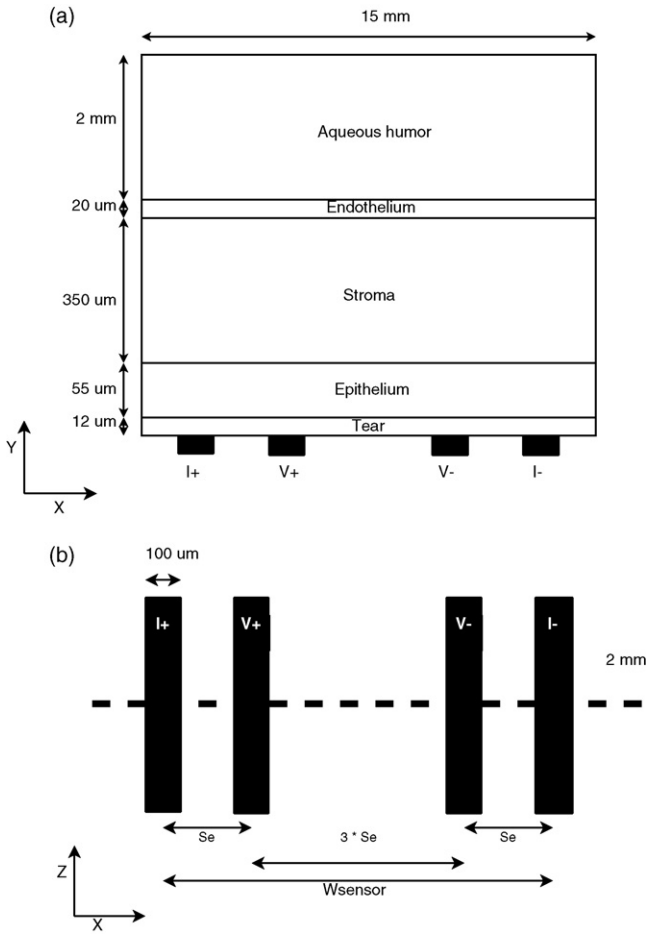


**Fig. 3.** (a) Schematic representation of the simulated model, which shows the modeled layers and the electrode placement. (b) Schematic representation of the simulated electrodes geometry. Where *I*+ and *I*− are the current electrodes, *V*+ and *V*− are the voltage sensing electrodes. The dashed line indicates position of the simulated vertical cross-section.

of the cornea (11 mm in diameter) and its curvature, so, 3 mm and 5 mm seem a reasonable compromise between the penetration of the measure and the cornea dimensions.

### 2.2. Corneal electrical properties

The electrical properties and thicknesses of the different modeled layers for a normal cornea are shown in Table 1. The physical dimensions of rabbit cornea have been taken into account, because rabbit is the reference animal model for *in vivo* eye experimentation. The tear layer has been defined with the electrical properties of the saline solution. Due to its lipid and mucous composition it is difficult to avoid the influence of this layer in the *in vivo* measurements. The thickness of this layer has been estimated to be around the 15 μm [17,18]. The epithelium layer has been modeled with the same electrical properties as the skin [19] due to their similar histological structure. The endothelium and stroma layer have been modeled according to the equivalent circuit proposed by Lim and Fischbarg [20] which is shown in Fig. 4. Considering the thickness of each layer, the resistivity values in $\Omega\,cm^2$ can be converted to conductivity values in S/m, needed for the simulation inputs. The aqueous humor has been modeled with the electrical properties of the saline solution [21].

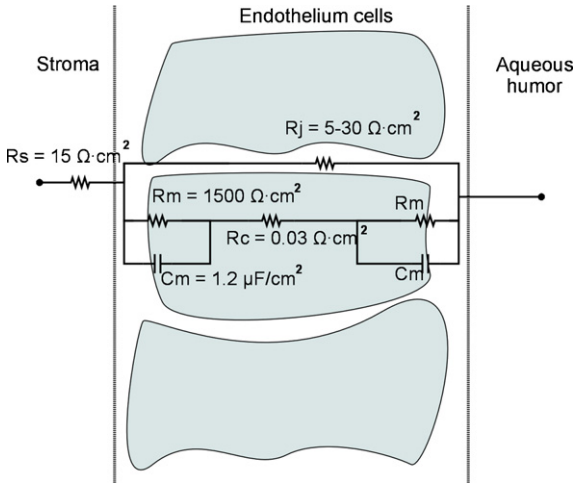


**Fig. 4.** Schematic morphological representation of the corneal endothelium with the corresponding equivalent electrical parameters at the postulated locations [20]. $R_m$, cellular membrane resistance; $R_s$, resistance of the stroma; $R_j$, resistance of the tight junctions; $R_c$, resistance of the cytoplasm; $C_m$, capacitance of the cell membrane.

### 2.3. Endothelial permeability model

For modeling the effect of endothelial damage on the passive electrical properties it has been assumed that the endothelium consists of a single monolayer of cells with intercellular spaces that are widened according to the amount of damage. Accordingly, Eq. (1) describes the relation between damage and conductivity of this layer.

$$\sigma_{\text{endothelium}} = \frac{\sigma_{\text{leak}}}{H} + \sigma_{\text{cells}} \quad \varepsilon_{\text{endothelium}} = \varepsilon_{\text{cells}} \tag{1}$$

where the parameter $H$ (for health status) would be inversely related to the amount of damage, $\sigma_{\text{leak}}$ represents the normal contribution of the intercellular spaces to the conductivity of the endothelium and $\sigma_{\text{cells}}$ and $\varepsilon_{\text{cells}}$ correspond to the conductivity and the permittivity of the endothelial cells respectively. Note that $\sigma_{\text{cells}}$ and $\varepsilon_{\text{cells}}$ depend on frequency whereas $\sigma_{\text{leak}}$ is frequency independent.

According to the reported changes of TER measurements when the endothelial permeability is pharmacologically increased [26,10], the simulated range values for parameter $H$ must range from 1 to 0.1 (1 represents the normal permeability; 0.1 is related with a decrease of 10% of the normal TER measurement). Fig. 5 shows the conductivity of the endothelial layer as function of the frequency for some values of parameter $H$.

### 2.4. Simulation strategy

In an actual clinical or experimental case, not only variations in the value of the endothelium permeability will be present but also the value for the other parameters of the model will be different from the normal case values displayed in Table 1. An increase in permeability of the endothelial layer can produce an alteration of the ionic concentration in the stroma layer and, as a result, a change of its conductivity. Moreover, an increase of endothelial permeability can also produce a variation of the stroma thickness due to the increment of the water content of this layer. On the other hand, the tear layer thickness can be modified by the sensor placement or by the ambient conditions. Therefore, in order to obtain a robust indicator insensitive to these uncontrollable variations, the effect of the endothelium conductivity on the measured impedance has been studied together with the variation of the other layers of the model. Table 2 shows the variations applied on the conductivity and thickness of the different layers.

**Table 1**
Values for the conductivity, permittivity and thickness of the modeled layers for a normal cornea.

| Layer | Conductivity [S/m] | Relative permittivity | Thickness [μm] | Ref. |
|---|---|---|---|---|
| Tear | 1.5 | 80 | 12 | [17,18,22] |
| Epithelium[a] | $4 \times 10^{-4}$ | $1 \times 10^{5}$ | 50 | [23–25] |
| Stroma | 0.2 | 80 | 350 | [20,24] |
| Endothelium[a] | $6.6 \times 10^{-3}$ | $1.3 \times 10^{4}$ | 20 | [20] |
| Aqueous humor | 1.5 | 80 | 2000 | [24] |

[a] Frequency depending values. These values correspond to 10 Hz.

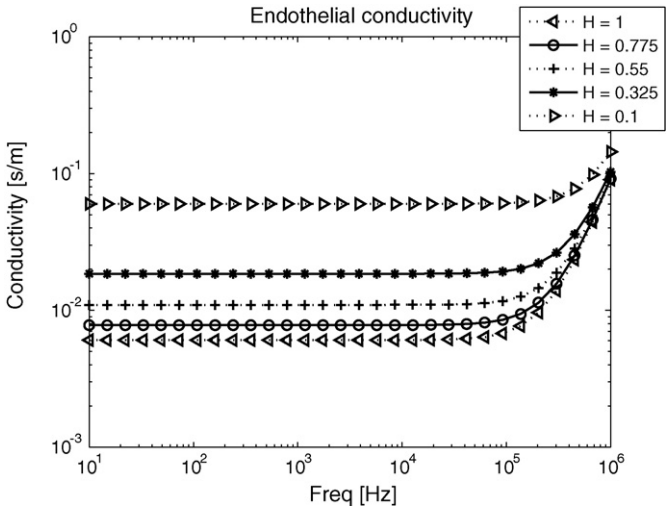


**Fig. 5.** Endothelial conductivity spectrogram for different values of parameter $H$ (inversely to the endothelial damage), evaluated according to Eq. (2).

### 2.5. Impedance sensitivity analysis

It can be defined a sensitivity parameter, $S$, that indicates the contribution of each infinitesimal volume of the sample to the total measured impedance. Such sensitivity parameter can be evaluated as follows [27,28].

$$S = \frac{\vec{J}_1 \vec{J}_2}{I^2} \tag{2}$$

where $S$ is the sensitivity to the conductivity changes at each location in the model, $\vec{J}_1$ is the current density vector when $I$ is injected between the two current electrodes, and $\vec{J}_2$ is the current density vector when the same current $I$ is injected between the two voltage sensing electrodes. Thus, the sensitivity at each location depends solely on the angle and magnitude of these two vectors and can be positive, negative or null. A positive value for the sensitivity means that, if the resistivity of this volume element is increased, a higher value of impedance is measured. A negative value means that, if the resistivity of this zone is increased, a lower value of impedance is measured. A higher absolute value for the sensitivity means a greater influence on the total measured impedance.

$$Z = \int_v \rho S dv \tag{3}$$

**Table 2**
Evaluated ranges for the conductivity and thickness of the modeled layers.

| Layer | Conductivity [S/m] | Thickness [μm] |
|---|---|---|
| Tear | 1.5 | 5–15 |
| Epithelium[a] | $2 \times 10^{-4}$ to $6 \times 10^{-4}$ | 55 |
| Stroma | 0.1–0.5 | 325–425 |

[a] Frequency depending values. These values correspond to 10 Hz.

$$\rho = \frac{1}{(\sigma + j\varepsilon_r \varepsilon_o w)} \tag{4}$$

The measured impedance $Z$ can be obtained as the integral of the sensitivity at each location weighted by the local complex resistivity $\rho$ over the volume $v$. The local complex resistivity value $\rho$ depends on the frequency and is defined as Eq. (4) [29]. Where $\sigma$ is the conductivity, $\varepsilon_r$ is the relative permittivity, $\varepsilon_o$ is the permittivity of the vacuum, and $\omega$ is the angular frequency. In the same way, the measured impedance due to each layer can be determined integrating each sub-volume $v_i$ corresponding to each layer.

$$Z_{v_i} = \int_{v_i} \rho S dv_i \tag{5}$$

$$\mathrm{Sel}_{v_i} = \frac{Z_{v_i}}{Z} = \frac{\int_{v_i} \rho S dv_i}{\int_v \rho S dv} \tag{6}$$

Another parameter, selectivity, was also analyzed in the present study [30]. It provides the impedance of each layer as a fraction of the total impedance measured and is defined in Eq. (6). In other words, it analyzes the ability of a given electrode arrangement to detect changes in the conductivity of the layer of interest. Therefore, this parameter is a convenient indicator for analyzing whether or not a set of electrodes is suitable to detect changes in the conductivity of the layer of interest.

## 3. Results

### 3.1. Simulation results from the impedance sensitivity analysis

Sensitivity map for the sensor with a width of 5 mm is presented in Fig. 6. The results for three different frequency values, 100 Hz, 6 kHz and 100 kHz, are shown. The represented zone corresponds only to the electrodes $V-$ and $I-$, because of symmetry. It can be observed a negative sensitivity zone between the voltage electrode and the current electrode. It is interesting to note that the sensitivity of the interior layers, stroma, endothelium and aqueous humor, is increased with the frequency range. On the other hand, the sensitivity at the external boundaries of the model is much lower than in the centre of the model. Thus, the assumption that tissues located beyond the limits of the model do not affect the impedance measurement can be considered true.

Fig. 7 shows the contribution of each layer to the total impedance as function of frequency. As expected, the contribution of each layer is different depending on the measured frequency. Three frequency ranges can be vaguely differentiated. At low frequencies the main contribution is due to the epithelium layer whereas at high frequencies the main contribution is due to the stroma layer and the aqueous humor layer. At intermediate frequencies, in a constrained frequency range, is where the endothelium layer reaches its maximum contribution. The approximate boundaries of these three behavioral frequency regions depend slightly on the sensor width. It is interesting to note that the

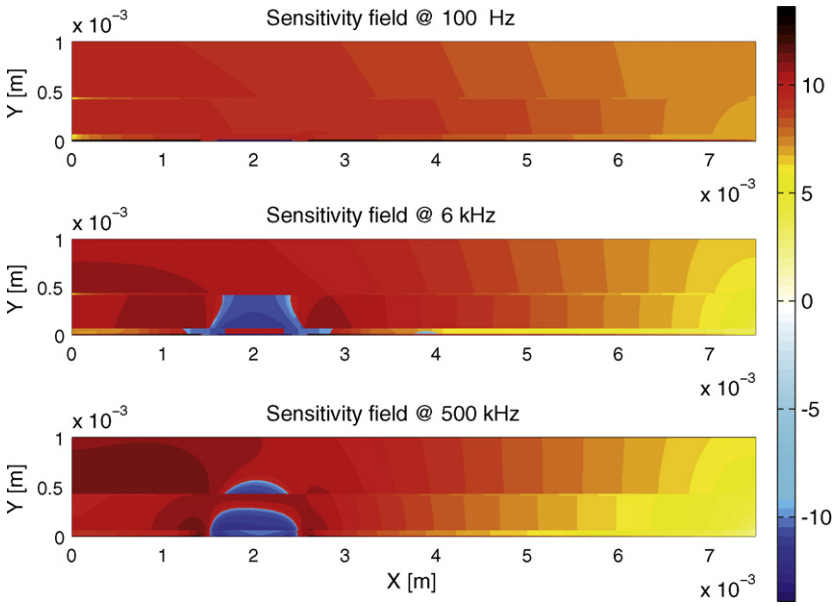


**Fig. 6.** Representation of the sensitivity field evaluated at three frequency points, 100 Hz, 6 kHz and 500 kHz. The sensitivity values are represented using a logarithmic scale color; positive sensitivities are visualized with a hot color map and negative with a cool color map.

contribution of the tear layer is considerable across the whole spectrum and that it has a negative contribution at frequencies above 1 kHz.

### 3.2. Simulation results when varying endothelial permeability

The results of these simulations are shown here in two ways: (1) the measured impedance in the frequency range from 10 Hz to 1 MHz and (2) the measured impedance at certain frequencies as function of the endothelial damage.

Fig. 8 shows the measured impedance for different values of the parameter *H*. It can be observed that the variation of this parameter affects the measured impedance at the frequency range from 2 kHz to 12 kHz. As expected, the measured impedance is lower when the damage in the endothelial layer is increased (parameter *H* is decreased) according to the higher conductivity of this layer. It is interesting to note that the variation is more significant with the sensor width of 5 mm.

Fig. 9 shows the effect of the stroma layer on the measured impedance. Two parameters of this layer have been studied: the stroma conductivity and the thickness. The effect of the changes in this layer is reflected at frequencies above 1 kHz, and is larger when the sensor of 3 mm is used. Fig. 10 shows the measured impedance for different values of tear layer thickness and epithelium conductivity. It can be observed that the variation of the epithelium conductivity only is reflected at frequencies below 1 kHz. On the other hand, the variations in the tear layer thickness are notable in all the frequency range.

Several simulations have been carried out for finding out the most reliable indicator of the endothelial damage. As mentioned, the effect of the endothelium conductivity has been simulated together with reasonable variations for the other parameters of the model. The studied parameters of the model and their simulated range values are shown in Table 2. For each studied parameter a five points parametric analysis has been performed. At each point of these analyses, other five values for the parameter *H* have been analyzed. Therefore, a total of 20 results have obtained. From all those results, a robust indicator (i.e. only related to the endothelial damage) was looked for. Fig. 11 shows the measured impedance modulus at 6 kHz function of the parameter *H*, which is inversely proportional to the endothelial damage. All simulation results are shown in a boxplot representation. It can be observed that these parameters are strongly related with the endothelial damage, but they have a significant dispersion. The dispersion is mainly caused by the variations of the stroma conductivity and tear layer thickness. In order to reduce the dispersion, two new indexes based in the measured impedance have been evaluated. Those indexes are presented and justified in Section 4.

## 4. Discussion

Observing the sensitivity results (Fig. 6), and the impedance contribution of the different layers (Fig. 7), three frequency zones can be easily differentiated. In the low frequency region (up to frequencies of about 1 kHz), the measurement is only affected by the tear layer and by the epithelium layer. This observation can be explained as being the result of the fact that the resistivity of the epithelium layer is very high in this frequency range and, therefore, the current cannot pass easily through it. Therefore, the measured voltage drop is only due to the resistivity of these two layers. It is worth noting that a similar effect has been reported in the case of skin impedance measurements [31]. The second zone of intermediate frequencies is limited in the frequency range from 1 kHz to 100 kHz. This zone can be defined as a transition zone, the contribution of the exterior layers is decreasing and the contribution of the interior layers is increasing. As can be observed, the maximum contribution of the endothelium layer is reached in this zone. Finally, the third zone corresponds to high frequency range; it can be defined by frequencies above 100 kHz. In this frequency range the conductivity of the cellular layers is very low and the current can pass through them easily. Therefore, the layers with major contribution to the measure are the thickest layers, the stroma and the aqueous humor.

Fig. 8 shows the measured impedance for the different values of parameter *H*. According to the study of the contribution of each layer, the variation of the endothelium conductivity is reflected in the frequency range from 2 kHz to 12 kHz. The analysis of the measured impedance at this frequency range is quite complex because multiple factors contribute to it. On one hand, the conductivity of the aqueous humor layer is larger than the conductivity of the stroma layer and, as consequence, the current will tend to

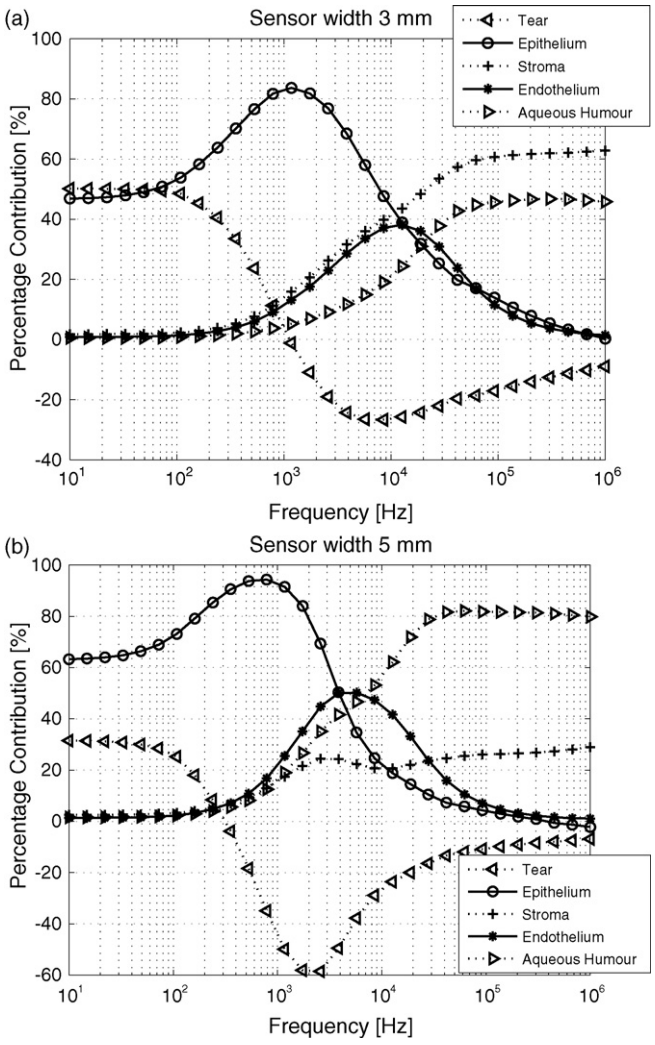


**Fig. 7.** Contribution of each layer to the total measured impedance as function of frequency for the two studied sensor width: (a) 3 mm and (b) 5 mm. Note that the contribution of each layer has a big dependence on frequency. At intermediate frequencies is where the endothelium layer reaches its maximum contribution.

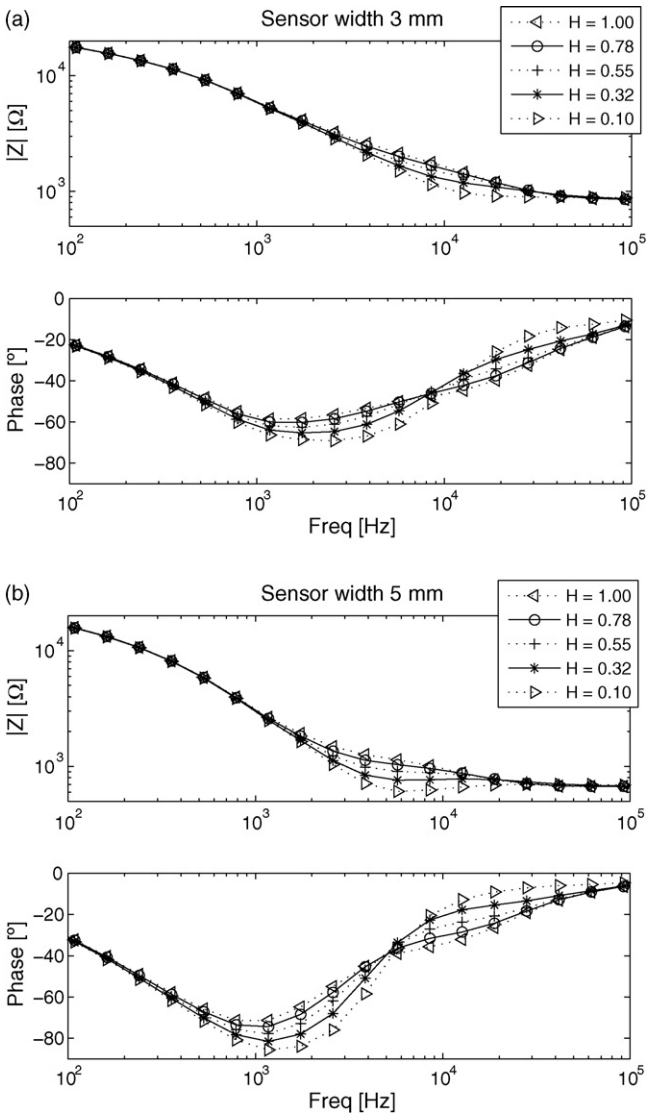


**Fig. 8.** Calculated impedance modulus and phase shift for different values of parameter $H$, showing the effect of the endothelial damage (inversely to parameter $H$) in the measured impedance for the two studied sensor widths: (a) 3 mm and (b) 5 mm. The major influence of the endothelial damage in the measured impedance is observed with a 5 mm sensor at the intermediate frequency range.

go through the aqueous humor. On the other hand, the amount of current than can pass from the stroma to the aqueous humor layer is modulated by the conductivity of the endothelium layer. Therefore, the decrease in the measured impedance is not only due to a decrease in the conductivity of the endothelium layer, but also due to an increase of the contribution of the aqueous humor. The profundity of the measurement is proportional to the separation of the electrodes. Hence the variation of the measured impedance due to changes in the conductivity of the endothelium layer is larger when electrodes of 5 mm width are used. The corneal impedance measurement presents two frequency dispersions, one due to the epithelial layer and another due to endothelial layer. The sensor width determines to some extent the frequency range of these two dispersions: a reduction of the sensor width produces an increase in the frequency of the epithelium dispersion, which ends up hiding the endothelium dispersion. Therefore, in order to observe the dispersion due to the endothelial layer and thereby to obtain information on its permeability, the sensor width has to be maximized. However, this parameter is limited by the size and curvature of the cornea. For this reason, the sensor width of 5 mm was the maximum size considered here.

The behavior of the impedance measurements of the cornea in relation to different model parameters has been studied. Physiological variations and changes due to the variation in the endothelial permeability have been modeled. For instance, it is known that an increase in the endothelium permeability leads to an increase in the level of the stroma hydration and this effect has been modeled by an increase of its conductivity due to an increment of its ionic concentration and by an increase of its thickness, due to a swelling produced by increment of water content. Moreover, other variations such in some modeled parameters, such as the conductivity of the epithelium and the thickness of the tear layer, have been introduced for modeling physiological variability. Table 2 shows the ranges of changes implemented in the model. Fig. 9 shows the effect of the stroma in the measured impedance, according with the sensitivity analysis, the changes in its conductivity and thickness can be observed in frequencies above 1 kHz. The thickness variation produces slight alterations in the measured impedance and its effect is noticeable in frequencies above 10 kHz. On the other hand, the alterations produced by the stroma conductivity are more important and have influence in the frequency range where the endothelium conductivity can be detected. The stroma conductivity variations have a more importance when a narrower sensor is used,

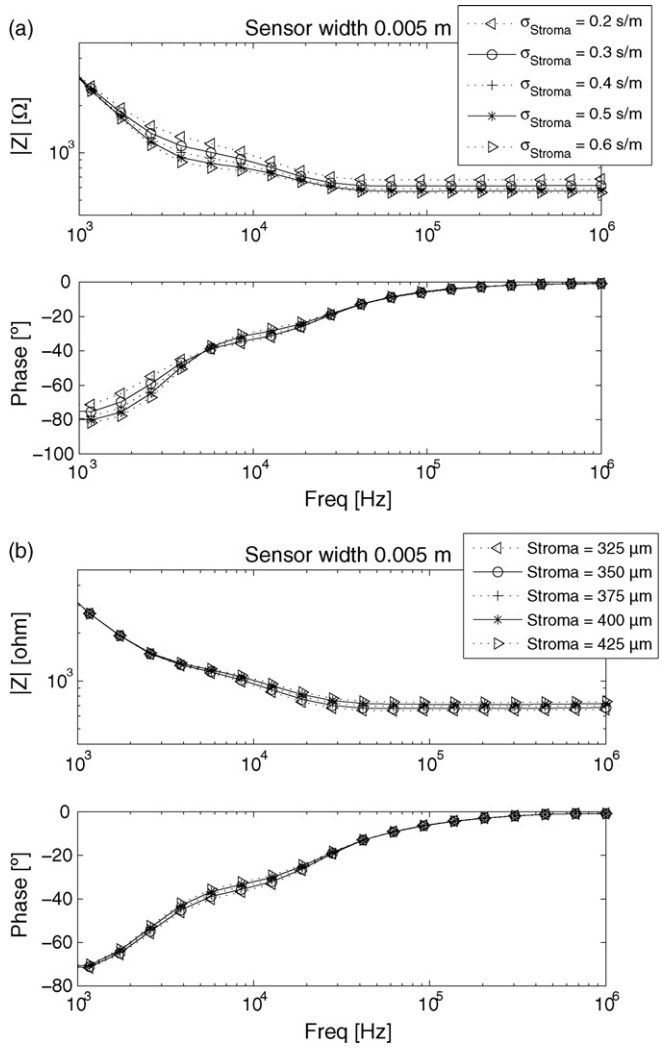


**Fig. 9.** Calculated impedance modulus and phase shift for different stroma conductivities and thickness values using a 5 mm width sensor (a) for different values of stroma conductivity (b) for different values of stroma thickness. The variation of the stroma conductivity implies an alteration of the measured impedance in the same frequency range where the endothelial damage can be detected. However, the stroma thickness variation only modifies the measured impedance at high frequencies.

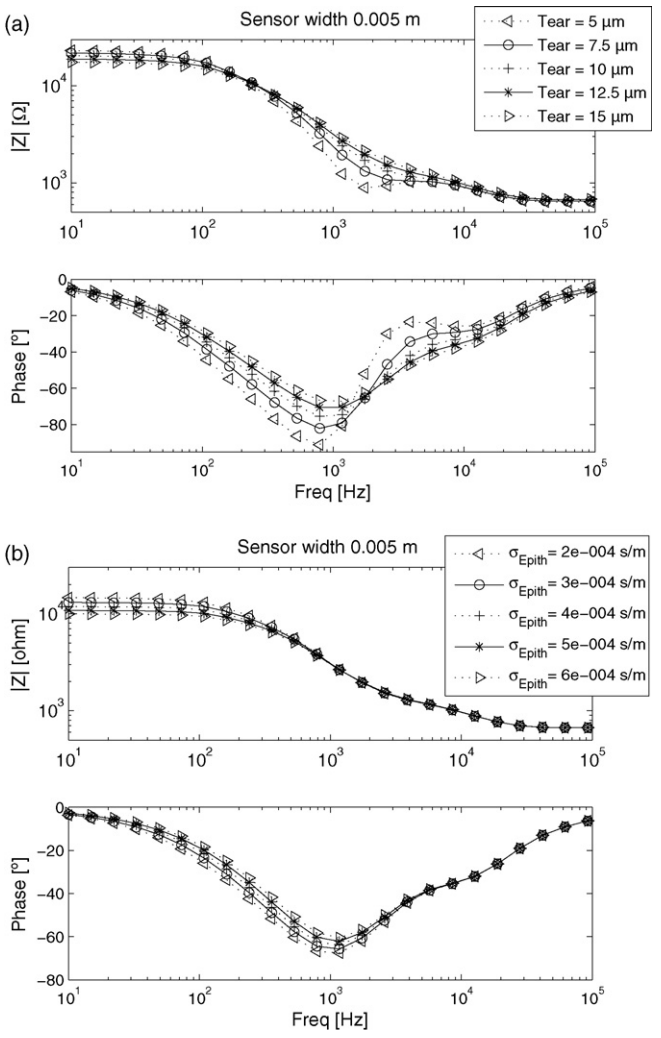


**Fig. 10.** (a) Calculated impedance modulus and phase shift of different values of tear thickness using a 5 mm width sensor. (b) Calculated impedance modulus and phase shift of different values of epithelium conductivity using a 5 mm width sensor. The variation of the tear thickness modifies the measured impedance at all frequencies. This alteration is very noticeable in the phase shift. However, the epithelium conductivity only modifies the measured impedance at the low frequency range.

because the contribution of this layer to the measured impedance is greater, as can be observed in Fig. 7. Finally, the simulations of the variations of the tear film thickness confirm that this layer has influence in the measured impedance in a large frequency range, from 10 Hz to 100 kHz (Fig. 10). As can be observed, the major influence of the tear thickness is on the phase shift measurement, reaching values minor than −90°. Apparently, this phase shift values are incongruous, but, they can be explained for the big difference of conductivity between tear film, the epithelium and the stroma. This fact produces two different paths for the current. This tends to go through the layers with lower conductivity, the tear film and the stroma. Thus, the measured voltage drop is mainly due to the current that goes through the tear film, but the measured impedance is evaluated over the total current. Grimnes and Martinsen [27] inform of this effect for explain strange values of phase shift in the case of skin impedance measurements when tetrapolar electrodes are used.

As we have mentioned, the physical dimensions of the model correspond to a rabbit cornea. After analyzing the results, we can discuss the feasibility of the results for a human cornea: the main structural difference between the human and the rabbit cornea is the thickness of the stroma layer, 350 μm for a rabbit and 500 μm for a human. The current penetration inside the model is much greater than the thickness of the cornea because the detection of the endothelial permeability is based on how this layer regulates the pass of current from stroma to aqueous humor. For this reason, qualitatively, the major part of the assumptions carried out in this paper should be valid in a human cornea.

In order to find out a robust indicator of the endothelium permeability, the effect of the variation of the endothelial conductivity on the impedance measurement has been analyzed together with changes in other parameters of the model detailed in Table 2. Apart from the endothelial conductivity, it has been modified: the tear film thickness, the epithelium conductivity, the stroma conductivity and the stroma thickness. For each of these 4 parameters, 5 points sweeps in the specified range have been simulated. For each point of these sweeps another 5 points nested sweep of the endothelial conductivity have been done. Thus, a total of 20 measurements for each evaluated endothelial conductivity value have been realized. On one hand, the relationship between the impedance modulus at 6 kHz and the endothelium conductivity have been studied, because this is the frequency where

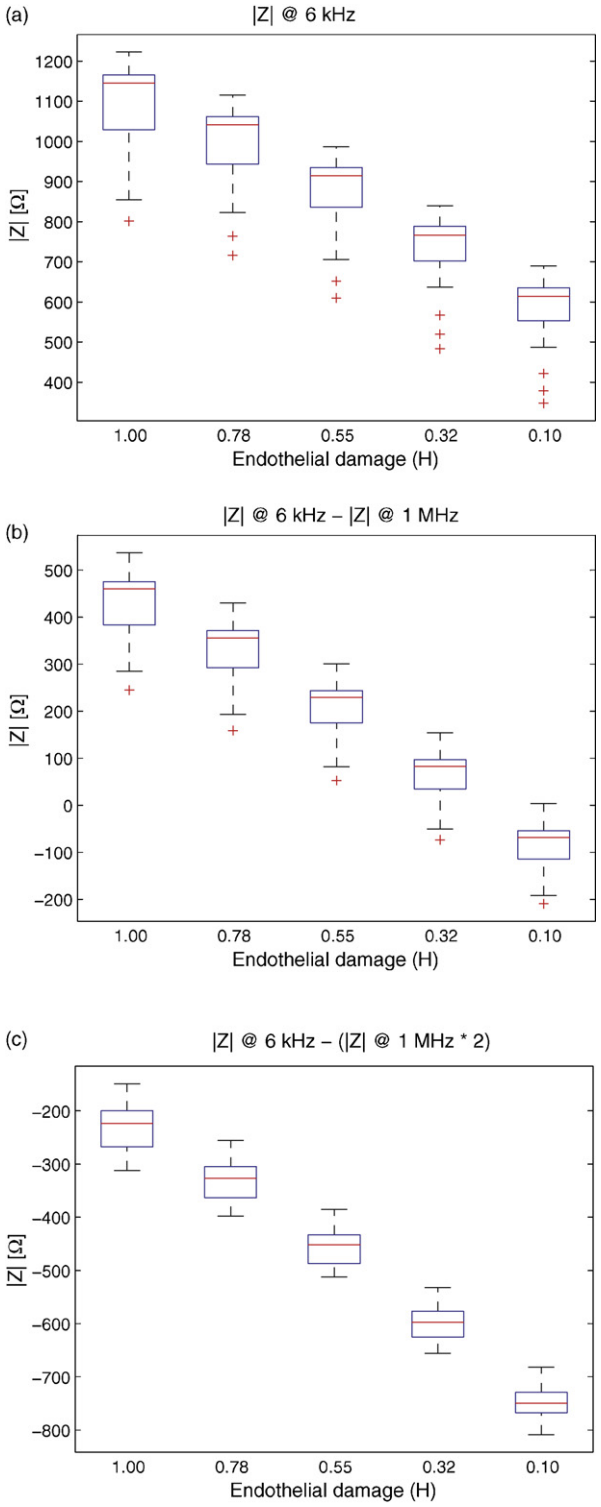


**Fig. 11.** Representation of the different presented indexes for the assessment of the endothelium permeability as a function of the endothelial damage (inversely proportional to parameter *H*). The effect of the endothelial damage is presented together with the other variations of the model parameters. The boxplot representation shows the mean value, the dispersion of the measures grouped by quartiles (boxes and bars) and the outliers values (as crosses). (a) Index based on the measured impedance modulus at 6 kHz, (b) index based on the measured impedance modulus at 6 kHz minus the measured impedance modulus at 1 MHz, (c) index based on the measured impedance modulus at 6 kHz minus the measured impedance modulus at 1 MHz scaled by a factor of 2. The measured impedance at 6 kHz presents a strong linear correlation with the endothelial permeability. The observed dispersion is mainly due to the variation of the tear thickness and the stroma conductivity. This dispersion can be reduced by subtracting the modulus impedance at 1 MHz.

the endothelial layer has a larger contribution to the measured impedance. On the other hand, the possibility of to compensate the dispersion produced by variations applied to the model has been studied. Represented in a boxplot Fig. 11a shows the measured impedance at 6 kHz as function of the parameter *H*, As can be observed, the modulus of the impedance at 6 kHz presents a strong linear correlation with the endothelial permeability, but also presents a big dispersion. This dispersion is mainly due to the variation of tear film thickness and of the stroma conductivity. A new index based on the impedance modulus measured at 6 kHz has been evaluated in order to reduce the dispersion observed. This index is obtained by subtracting the modulus of impedance at 1 MHz and the impedance modulus to 6 kHz. At 1 MHz, the main contribution to the measured impedance is due to the stroma layer and the aqueous humor. Therefore, the physical justification for the proposed index is to try to cancel the effect of the stroma layer on the measured impedance at 6 kHz, so that this index will only depend on the variation of the endothelium conductivity. As can be observed in Fig. 11b, the reduction of dispersion is notable, but not sufficient. So that, the value measured at 1 MHz is scaled up by a factor of 2 in order to compensate the different contributions of the layers along the frequency range. As shown in Fig. 11c, the results obtained with the latter indicator are acceptable, since the overlaps between data sets are minimal.

## 5. Conclusions

In this paper, we have evaluated the influence of the corneal endothelium permeability in the measurements of the corneal impedance by using FEM simulations. From the measured impedance by means of four electrodes placed on the cornea surface, it was found that the variation in the endothelium permeability can be detected. Furthermore, it was found that the impedance measurement is also influenced by the other layers of the cornea. But, it was found an indicator based on the impedance measurement of the cornea that is only related to the electrical properties of the endothelium. Thus, we conclude that the method presented here can be used as a non-invasive method for assessing endothelium layer function. This new method could be used in the clinical practice, filling the existing lack of this kind of methods.

## Acknowledgment

This work has been funded by the project SAF2009-14724-C02-02 from the Spanish Ministry of Science and Innovation.

## Conflict of interest

The authors have no financial or personal relationships with other people or organizations that could inappropriately influence or bias their work.

## References

[1] Fischbarg J, Hernandez J, Liebovitch LS, Koniarek JP. The mechanism of fluid and electrolyte transport across corneal endothelium: critical revision and update of a model. Curr Eye Res 1985;4(4):351–60.
[2] Fischbarg J, Diecke F. A mathematical model of electrolyte and fluid transport across corneal endothelium. J Membr Biol 2005;203(1):41–56.
[3] Jones R, Maurice D. New methods of measuring the rate of aqueous flow in man with fluorescein. Exp Eye Res 1966;5(3):208–20.
[4] Bourne WM, McLaren JW. Clinical responses of the corneal endothelium. Exp Eye Res 2004;78(3):561–72.
[5] McNamara N, Fusaro R, Brand R, Polse K, Srinivas S. Measurement of corneal epithelial permeability to fluorescein. A repeatability study. Invest Ophthalmol Vis Sci 1997;38(9):1830–9.
[6] Módis LÁ, Langenbucher A, Seitz B. Corneal endothelial cell density and pachymetry measured by contact and noncontact specular microscopy. J Cataract Refract Surg 2002;28(10):1763–9.

[7] Imre L, Nagymihály A. Reliability and reproducibility of corneal endothelial image analysis by in vivo confocal microscopy. Graefes Arch Clin Exp Ophthalmol 2001;239(5):356–60.
[8] Lass JH, Sugar A, Benetz BA, Beck RW, Dontchev M, Gal RL, et al. Endothelial cell density to predict endothelial graft failure after penetrating keratoplasty. Arch Ophthalmol 2010;128(1):63–9.
[9] Fischbarg J. Active and passive properties of the rabbit corneal endothelium. Exp Eye Res 1973;15(5):615–38.
[10] Ma L, Kuang K, Smith RW, Rittenband D, Iserovich P, Diecke F, et al. Modulation of tight junction properties relevant to fluid transport across rabbit corneal endothelium. Exp Eye Res 2007;84(4):790–8.
[11] Uematsu M, Kumagami T, Kusano M, Yamada K, Mishima K, Fujimura K, et al. Acute corneal epithelial change after instillation of benzalkonium chloride evaluated using a newly developed in vivo corneal transepithelial electric resistance measurement method. Ophthalmic Res 2007;39(6):308–14.
[12] Chetoni P, Burgalassi S, Monti D, Saettone MF. Ocular toxicity of some corneal penetration enhancers evaluated by electrophysiology measurements on isolated rabbit corneas. Toxicol In Vitro 2003;17(4):497–504.
[13] Schwan HP, Ferris CD. Four-electrode null techniques for impedance measurement with high resolution. Rev Sci Instrum 1968;39(4):481–5.
[14] Dewarrat F, Falco L, Caduff A, Talary M. Optimization of skin impedance sensor design with finite element simulations. In: COMSOL conference 2008, Hannover. 2008.
[15] Ivorra A, Aguiló J, Millán J. Design considerations for optimum impedance probes with planar electrodes for biomimpedance measurements. In: Semiconductor conference, 2001. CAS 2001 proceedings international. 2001.
[16] Robillard PN, Poussart D. Spatial resolution of four electrode array. Biomed Eng IEEE Trans 1979;26(8):465–70.
[17] López García JS, García Lozano I, Martínez Garchitorena J. Estimación del grosor de la capa lipídica lacrimal mediante colores interferenciales en distintos tipos de ojo seco. Archivos de la Sociedad Española de Oftalmología 2003;(5):257–64.
[18] Prydal J, Artal P, Woon H, Campbell F. Study of human precorneal tear film thickness and structure using laser interferometry. Invest Ophthalmol Vis Sci 1992;33(6):2006–11.
[19] Gabriel C, Gabriel S, Corthout E. The dielectric properties of biological tissues: I. Literature survey. Phys Med Biol 1996;41(11):2231–50.
[20] Lim J, Fischbarg J. Electrical properties of rabbit corneal endothelium as determined from impedance measurements. Biophys J 1981;36(3):677–95.
[21] Jurgens I, Rosell J, Riu PJ. Electrical impedance tomography of the eye: in vitro measurements of the cornea and the lens. Physiol Measure 1996;17(4A):A187–95.
[22] King-Smith PE, Fink BA, Fogt N, Nichols KK, Hill RM, Wilson GS. The thickness of the human precorneal tear film: evidence from reflection spectra. Invest Ophthalmol Vis Sci 2000;41(11):3348–59.
[23] Li HF, Petroll WM, M\oller-Pedersen T, Maurer JK, Cavanagh HD, Jester JV. Epithelial and corneal thickness measurements by in vivo confocal microscopy through focusing (CMTF). Curr Eye Res 1997;16(3):214–21.
[24] Gabriel S, Lau RW, Gabriel C. The dielectric properties of biological tissues: III. Parametric models for the dielectric spectrum of tissues. Phys Med Biol 1996;41(11):2271–94.
[25] Klyce SD. Electrical profiles in the corneal epithelium. J Physiol 1972;226(2):407–29.
[26] Bonanno JA. Identity and regulation of ion transport mechanisms in the corneal endothelium. Prog Retin Eye Res 2003;22(1):69–94.
[27] Grimnes S, Martinsen OG. Sources of error in tetrapolar impedance measurements on biomaterials and other ionic conductors. J Phys D: Appl Phys 2007;40(1):9–14.
[28] Geselowitz DB. An application of electrocardiographic lead theory to impedance plethysmography. Biomed Eng IEEE Trans 1971;18(1):38–41.
[29] Grimnes S, Martinsen OG. Bioimpedance and bioelectricity basics. Academic Press; 2008.
[30] Yang F, Patterson RP. A simulation study on the effect of thoracic conductivity inhomogeneities on sensitivity distributions. Ann Biomed Eng 2008;36(5):762–8.
[31] Martinsen OG, Grimnes S, Haug E. Measuring depth depends on frequency in electrical skin impedance measurements. Skin Res Technol 1999;5:179–81.